https://doi.org/10.5194/tc-2020-330
Preprint. Discussion started: 25 November 2020

The Cryosphere Discussions

Assessment of ICESat-2 ice surface elevations over the CHINARE route, East Antarctica, based on coordinated multi-sensor observations

Rongxing Li[1,2*], Hongwei Li[1,2], Tong Hao[1,2*], Gang Qiao[1,2], Haotian Cui[1,2], Youquan He[1,2], Gang Hai[1,2], Huan Xie[1,2], Yuan Cheng[1,2], Bofeng Li[1,2]

[1]Center for Spatial Information Science and Sustainable Development and Applications, Tongji University,
[2]College of Surveying and Geo-informatics, Tongji University, Shanghai 200092, China

Correspondence to: Rongxing Li (rli@tongji.edu.cn)

Abstract. This paper presents the results of the assessment of ICESat-2 ice surface elevations along the CHINARE (CHINese Antarctic Research Expedition) route in East Antarctica. The validation campaign was designed and implemented in cooperation with the 36th CHINARE Antarctic expedition from December 2019 to February 2020. The assessment of the ICESat-2 ATL03 and ATL06 data was performed based on coordinated multi-sensor observations using two roof-mounted kinematic GNSS receivers, two line arrays of corner cube retroreflectors (CCRs), two sets of retroreflective target sheets (RTSs), and two unmanned aerial vehicles (UAVs) with cameras. This systematic validation of the ICESat-2 data covered a variety of Antarctic ice surface conditions along the 520 km traverse from the coastal Zhongshan Station to the inland Taishan Station. This comprehensive investigation is complementary to the 750 km traverse validation of flat inland Antarctica containing a 300 km latitude traverse of 88 °S by the mission team in a previous study. Overall, the validation results show that the elevation of the ATL06 ice surface points is accurate to 1.1 cm with a precision of 9.7 cm along the 520 km CHINARE route. The elevation of the ATL03 photons has an offset of 2.4 cm from a GNSS-surveyed CCR, and is accurate to 2.5 cm with a precision of 2.7 cm as estimated by using RTSs. The validation results demonstrate that the estimated ICESat-2 elevations are accurate to 1.1–2.5 cm in this East Antarctic region, which is important for overcoming the uncertainties in the estimation of mass balance in East Antarctica. The developed validation methodology and sensor system can be improved for continuous assessment of ICESat-2 data, especially during the later operation period.

1 Introduction

The Ice, Cloud, and Land Elevation Satellite-2 (ICESat-2) using the new photon-counting technology was successfully launched by the National Aeronautics and Space Administration (NASA) on September 15, 2018 (National Research Council, 2007; Markus et al., 2017; Neumann et al., 2019). It is a follow-up to the previous ICESat laser altimetry mission, which is based on the full waveform ranging (Zwally et al., 2002; Schutz et al., 2008). The primary scientific objective of the ICESat-2 mission is to determine ice sheet height changes through continuous measurements at scales from the outlet glaciers to the

https://doi.org/10.5194/tc-2020-330
Preprint. Discussion started: 25 November 2020

entire ice sheet (Markus et al., 2017). As the single instrument onboard ICESat-2, the Advanced Topographic Laser Altimeter System (ATLAS) is a photon-counting laser altimeter using 532 nm wavelength laser pulses, which is designed to conduct surface-elevation observations at centimeter-level accuracy and is expected to reduce the uncertainty of the estimated sea level rise contribution from Antarctica (Markus et al., 2017; Neumann et al., 2018, 2019). More specifically, ICESat-2 aims to improve the accuracy of the elevation change rate to 0.4 cm a^{-1} (Markus et al., 2017; Smith et al., 2020). The ICESat-2 data collected during its initial and nominal mission periods up to November 2020 (at the time of this submission), including ice surface elevations of returned photons (ATL03) and those of estimated surface points (ATL06) on the Antarctic Ice Sheet (AIS), have been released to the public (Release 003; Neumann et al., 2019; Smith et al., 2019).

Calibration and validation campaigns are important for satellite altimetry missions, especially for the assessment of ICESat-2 performance with new photon-counting technology. Prior to launch, several airborne lidar experiments were carried out to validate this new satellite altimetry technology (Brunt et al., 2017; Magruder and Brunt, 2018). The results showed that surface-elevation biases for the tested altimeters, including the Multiple Altimeter Beam Experimental lidar (MABEL), over the flat ice sheet interior are less than 0.12 m with a precision of 0.09 m or better (Brunt et al., 2017). After launch, the mission team conducted a 750 km traverse validation of flat inland Antarctica containing a 300 km latitude traverse of 88 °S from December 31, 2018 to January 11, 2019 using kinematic Global Navigation Satellite Systems (GNSSs) to assess the elevation and horizontal accuracy of the ICESat-2 data products (Release 001) on AIS (Brunt et al., 2019b). These results indicated that ATL03 data (Release 001) are accurate to 5 cm of surface elevation with a precision of 13 cm, while ATL06 data (Release 001) are accurate to 3 cm with a precision of 9 cm. The team also used a corner cube retroreflector (CCR) array to collect ICESat-2 signatures and a horizontal geolocation accuracy of 2–5 m was achieved; additionally, the average beam diameter was estimated as ~11 m (Neumann et al., 2020b). Although this ICESat-2 validation campaign covered a long traverse of the flat Antarctic interior along the latitude of 88 °S, additional coverage containing the lower-latitude interior and coastal regions in AIS should make the validation of ICESat-2 data complete with an ample and comprehensive understanding of elevation of the whole AIS. More specifically, such a validation in East Antarctica should help confirm the regional ICESat-2 surface elevation accuracy with which it is expected to eliminate or reduce the uncertainty of the mass balance and change rate in East Antarctica (Zwally et al., 2015; Scambos and Shuman, 2016; Richter et al., 2016).

To assess the accuracy of the Antarctic surface elevations provided in the ICESat-2 ATL03 and ATL06 data products and their capability for the estimation of the mass balance of AIS, complementary to the current validation efforts by the mission team, we designed and implemented an independent validation campaign based on a set of coordinated multi-sensor experiments along the 520 km 36th CHINARE (CHINese Antarctic Research Expedition) route in East Antarctica from December 2019 to February 2020 (Fig. 1). The ground sensors used in this coordinated validation campaign include five GNSS master receivers on the ice surface serving as base stations, two roving GNSS receivers on a snowcat, two sets of CCRs, two sets of retroreflective target sheets (RTSs), and two unmanned aerial vehicles (UAVs) with cameras. Five GNSS base stations with CHC i70 receivers from CHC Navigation Technology LTD (http://www.huace.cn/product/product_show/291) were deployed every ~100 km along the CHINARE route from the coastal Zhongshan Station to the inland Taishan Station to support the two

https://doi.org/10.5194/tc-2020-330
Preprint. Discussion started: 25 November 2020

roving GNSS receivers (CHC i70) installed on roof of a snowcat, Pisten Bully Polar 300, for a real-time kinematic (RTK) positioning survey. Two sets of ten upward-looking CCRs (optical prisms) were deployed at sites near Zhongshan Station and Taishan Station, respectively, to capture photons for the verification of individual reflected photons with a known elevation. We used one rectangular (5 m × 150 m) RTS for each site to investigate the reflectivity and elevation accuracy of photons reflected from selected RTS coatings. Finally, two UAVs, DJI Phantom 4 (https://www.dji.com/cn/phantom-4-rtk?site=brandsite&from=nav), were used to acquire images for the generation of digital elevation models (DEMs) with centimeter accuracy for the assessment of ICESat-2 elevation accuracy. The campaign initially included the Great Wall Station as the third site, where the CCRs and RTSs were planned to be used. Due to logistic difficulties during the Covid-19 pandemic, the experiments at this site were cancelled, which unfortunately affects the completeness of our planned geographic coverage. Nevertheless, our calibration and validation work at Zhongshan Station and Taishan Station can provide in-depth knowledge of ICESat-2 surface elevation accuracy taking into account various terrain characteristics of coastal and inland Antarctica.

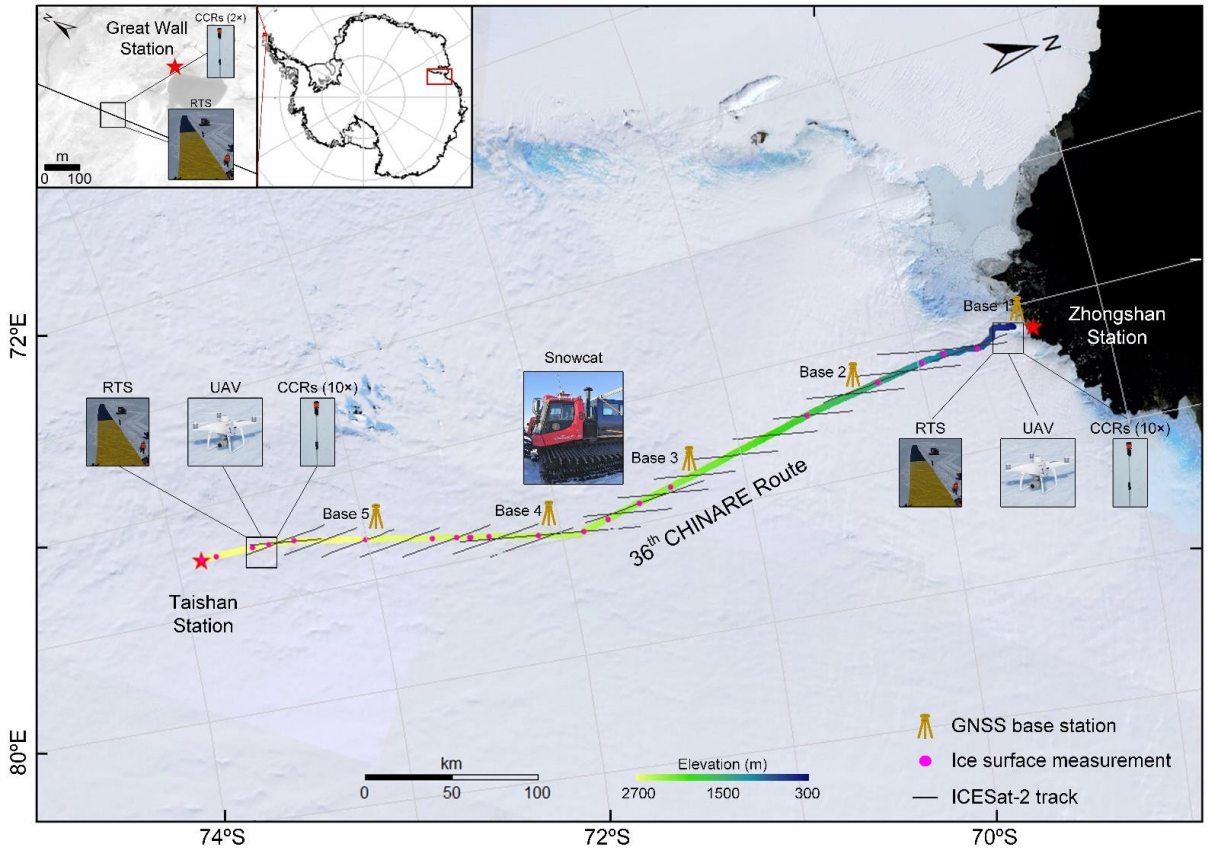

Figure 1. ICESat-2 validation campaign based on coordinated multi-sensor ground observations along the 36th CHINARE route. The Landsat image mosaic of Antarctica (Bindschadler et al., 2008) is used as main background and WorldView 2 image as the inset background.

https://doi.org/10.5194/tc-2020-330
Preprint. Discussion started: 25 November 2020


The Cryosphere Discussions

2 Data

The ICESat-2 Release 003 data used for ground validation in this study are L2A Global Geolocated Photon Data (ATL03) and L3A Land Ice Height data (ATL06; Neumann et al., 2019; Smith et al., 2019) collected along 60 ascending and 78 descending tracks between November 10, 2019 and February 21, 2020 (Table 1).

Table 1. Summary of the ICESat-2, GNSS and UAV observations used in this study.

Data type	Acquisition date (UTC)	Number of observations	Resolution	Geolocation accuracy	Format	Source
Data for ICESat-2 ATL03 and ATL06 validation along GNSS traverse						
ICESat-2 ATL03 Release 003	2019-11-10 to 2020-02-21	20,562 photons	~0.7 m spacing	planimetric: 2–5 m	HDF5	NSIDC
ICESat-2 ATL06 Release 003	2019-11-10 to 2020-02-21	758 points	~20 m spacing	not applicable	HDF5	NSIDC
GNSS observations along traverse	2019-12-10 to 2020-02-14	625,358 points	~4 m spacing	vertical: 0.1 ± 5.5 cm	binary	this study
Additional data for ICESat-2 ATL03 validation based on CCRs and RTSs						
GNSS observations at CCRs and RTSs near Zhongshan Station	2020-01-22	137 points	at CCRs and distributed on RTSs	vertical: 0.4 cm	binary	this study
GNSS observations at CCRs near Taishan Station	2020-01-23	10 points	at CCRs	vertical: ~1 m	binary	this study
Additional data for ICESat-2 ATL06 validation based on UAV-DEM						
UAV image orthophoto near Zhongshan Station	2020-01-22	154 scenes	~4.6 cm	1.3 cm	GeoTIFF	this study

We collected a total of ~1008 km (~516 km inbound and ~492 km outbound) of kinematic GNSS survey data during the 36th CHINARE inland expedition between Zhongshan Station and Taishan Station (Fig. 1), using two roving GNSS receivers mounted on roof of the snowcat (Fig. 4a). The GNSS receivers obtained data from the Global Positioning System (GPS), GLObal NAvigation Satellite System (GLONASS), Galileo Global Navigation Satellite System (Galileo), and BeiDou Navigation Satellite System (BDS). Along the inbound traverse journey (December 10–15, 2019), five GNSS base stations were deployed with ~100 km spacing. Base 1 was located on the roof of a container near the runway of the Russian Progress Station and the other four stations were installed on the ice surface during the traverse. During the outbound traverse (February 8–14, 2020), we only used Base 1 (AC powered) since the other four stations had run out of battery after the inbound traverse trip. The sampling rate was set to 1 Hz to conserve the power and storage space, and the elevation angle mask was set to 7 °to reduce the multipath effect. The same settings were also applied for the roving GNSS receivers. The RTK processing resulted in a vertical accuracy of 0.1 ±5.5 cm for the roving GNSS receivers.

https://doi.org/10.5194/tc-2020-330
Preprint. Discussion started: 25 November 2020

The Cryosphere Discussions

Ten CCRs of 6 cm diameter (Fig. A1a) were placed linearly at a 10 m interval across a nominal ICESat-2 ground track to capture photons from ATLAS (Fig. 2a). To mitigate the error induced by the possible subsidence of the aluminum pole supporting each CCR, a wood base (40 cm × 40 cm × 1 cm) was assembled at the bottom of each pole. The elevations of the nominal centers of the CCR lens near Zhongshan Station were measured by an RTK survey with a vertical accuracy of 0.4 cm. Due to logistic difficulties, the CCRs near Taishan Station were surveyed using the single-point positioning technique with a vertical accuracy of ~1 m.

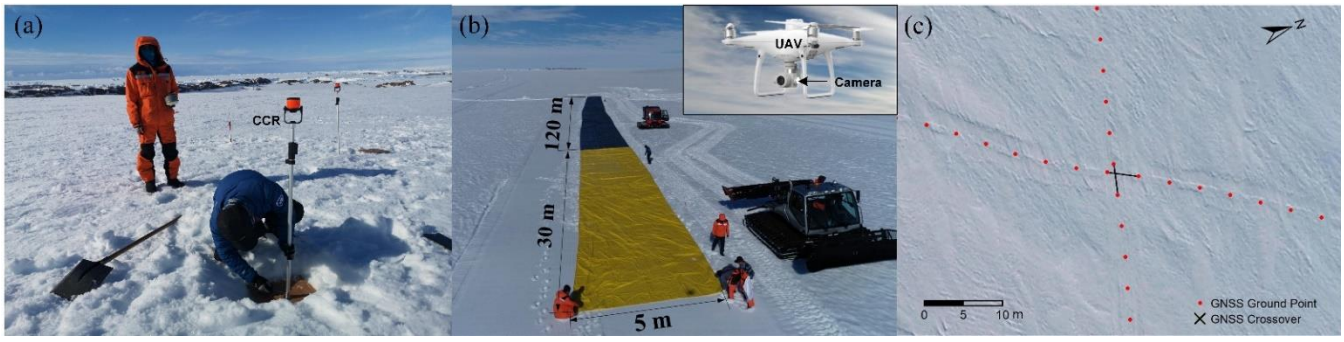

Figure 2. (a) Ten CCRs were installed along a line across an ICESat-2 ground track at each site; (b) a two-coating RTS (5 m × 150 m with yellow and dark green coatings) was deployed near Zhongshan Station and surveyed by a UAV; and (c) example of a GNSS crossover point and snowcat tracks on a UAV image.

RTSs were designed to assess the reflectivity and elevation accuracy of the ICESat-2 photons from a known artificial surface in the Antarctic environment. We deployed an RTS of 5 m × 150 m at each site, which was oriented perpendicular to the two ICESat-2 tracks (weak and strong), that is ~90 m apart. An RTK GNSS survey of 137 randomly distributed points on the RTS near Zhongshan Station was performed. The coatings of the RTSs were selected from among 28 candidates through a pre-expedition experiment. For each coating, an Avafield-3 spectrometer (https://www.avantes.com/products/spectrometers/compactline) was used to measure the reflectivity (R) of each coated RTS at the ICESat-2 wavelength of 532 nm; we also used a lidar ranger of Riegl BDF-1 (http://www.riegl.com/uploads/tx_pxpriegldownloads/RIEGL_BDF-1_Datasheet_2019-05-31.pdf) with a laser wavelength of 532 nm to measure the corresponding reflectance (r). We selected the silver–gray coating with R = 0.235 which is closest to R = 0.28 which has reportedly the highest estimated probability (EP) of photon detection (Hartzell et al., 2018). We added two other coatings, i.e., yellow (R = 0.532) for high reflectivity and dark green (R = 0.060) for low reflectivity. Thus, the RTS near Zhongshan Station had yellow and silver–gray coatings, while the one near Taishan Station had yellow and dark green coatings. A UAV equipped with an HD camera (1″ CMOS, 20 megapixel) was flown over an area of 750 m × 500 m near Zhongshan Station. A total of 154 images were collected with an along-track overlapping of 80% and a side overlapping of 75%. At a flight height of ~250 m the ground resolution was 4.6 cm. The CCRs and RTS were inside the mapping area. A high-precision GNSS survey was carried out for photogrammetric processing and DEM reconstruction.

https://doi.org/10.5194/tc-2020-330
Preprint. Discussion started: 25 November 2020

3 Method

As shown in Fig. 3, this Antarctic validation campaign was designed to achieve three goals: a) assessment of ICESat-2 surface elevations (ATL03 and 06) using a kinematic GNSS survey along the 520 km CHINARE route (69.46–73.86° S); b) assessment of elevations of the targeted ICESat-2 photons (ATL03) from the CCRs and RTSs; and c) assessment of ICESat-2 elevations (ATL06) using a UAV survey. The major steps of processing are illustrated in Fig. 3.

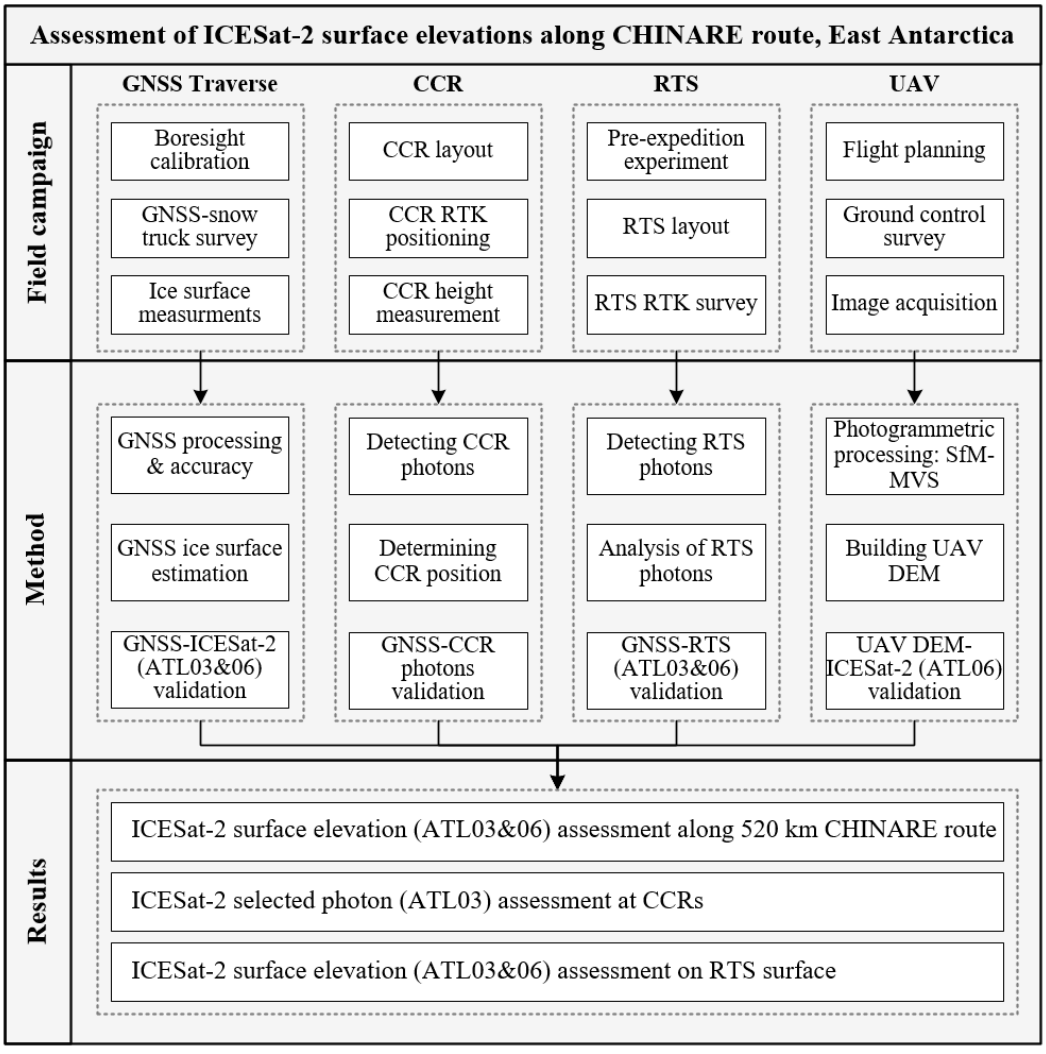

Figure 3. Flow chart for assessment of ICESat-2 ice sheet surface elevations along the CHINARE route as well as two validation sites, East Antarctica, based on coordinated multi-sensor observations.

https://doi.org/10.5194/tc-2020-330
Preprint. Discussion started: 25 November 2020

3.1 Kinematic GNSS – ICESat-2 ice surface elevation validation

3.1.1 GNSS data processing

Each GNSS base station was deployed before the snowcat started its ~100 km survey along the inbound traverse (Fig. 1). The master receivers collected data from GPS, GLONASS, Galileo, and BDS systems during the batteries' lifetime (~3 days), except Base 1 (all days, powered by AC). The double-frequency data were post processed using the precise point positioning (PPP) technique implemented in the software system of multi-frequency and multi-system instantaneous PPP (MUSIP) developed at Tongji University (Li et al., 2019), with the precise ephemeris and clock products provided by GFZ (ftp://ftp.gfz-potsdam.de/GNSS/products/mgex). Two roving receivers, Antenna 1 and Antenna 2, were mounted on the roof of the snowcat (Fig. 4). Combined with the PPP results of the base stations, GNSS data collected by the roving receivers along the traverse were handled using the post-processed kinematic (PPK) positioning technique that is implemented in an open source software package RTKLIB version 2.4.3 (http://www.rtklib.com/) developed by the Laboratory of Satellite Navigation at Tokyo University of Marine Science and Technology (Takasu et al., 2009; Takasu, 2013). The snowcat positions within a segment of up to ~90 km from each base station were estimated.

In addition to the precision of the estimated snowcat positions given by the software system, we used the accuracy computed from elevation differences at crossovers where the GNSS surveyed track intersected itself, as shown in Fig. 2c. These crossovers are the intersections of tracks by the snowcat during instrument installations, observations, and overnight breaks. Within a neighborhood of the intersection we fit two lines to compute the crossover location and elevation difference (Kohler et al., 2013).

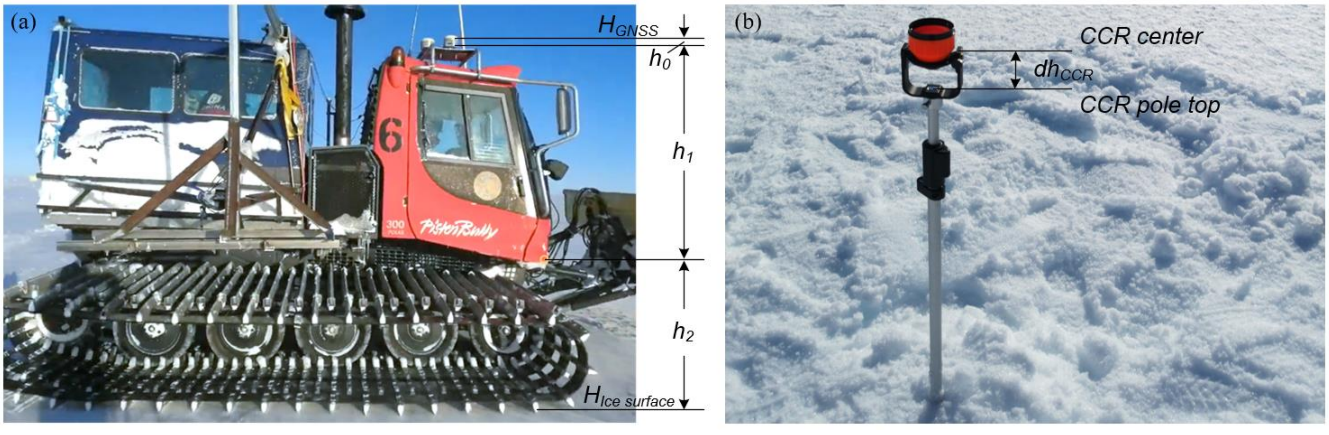

Figure 4. (a) GNSS roving receivers mounted on the roof of a Pisten Bully snowcat and boresight parameters for ice surface elevation estimation from the GNSS observations, and (b) CCR installed in the field with the pole top elevation ($h_{Pole\ top}$) surveyed by GNSS and the CCR center height (dh_{CCR}) measured using a steel tape.

https://doi.org/10.5194/tc-2020-330
Preprint. Discussion started: 25 November 2020

3.1.2 Derivation of ice surface elevations from GNSS observations

Given the antenna phase-center elevation of a roof-mounted GNSS roving receiver H_{GNSS} (Fig. 4a), the elevation of the ice surface can be computed as

$$H_{Ice\ surface} = H_{GNSS} - h_0 - h_1 - h_2\ , \quad (1)$$

where h_0 is the antenna phase-center height above the mounting plane and h_1 is the vertical distance between the mounting plane and a reference point marked by a yellow dot on the snowcat in Fig. 4a, from which the vertical distance to the ice surface h_2 can be measured. h_0 was given by the manufacturer as 10.1 cm. Prior to the GNSS traverse survey, a boresight calibration was performed to estimate the fixed parameter h_1. We used a SOKKIA CX-102LN total station to measure h_1 three times and estimated an average of 191.1 cm. During the breaks along the traverse we used a steel tape to measure h_2. To reduce measurement error due to the uneven ice surface, we measured it three times across a section with an interval of 10 cm. Thus, wherever h_2 is measured, the ice surface elevation $H_{Ice\ surface}$ can be computed from the roving receiver observation H_{GNSS} and the boresight parameters h_0 and h_1.

3.1.3 Ice surface elevation comparison along the GNSS traverse

Each ICESat-2 orbit has three pairs of ground tracks (1, 2 and 3 in Fig. 5a) which is 3 km apart (ICESat-2 Technical Specs, 2020). Each track pair corresponds to two laser beams, L (left) for weak beam and R (right) for strong beam. This correspondence may change as the ATLAS system changes its orientation. For example, an ascending ICESat-2 orbit (six tracks) intersected the CHINARE route (red line) at ~420 km from Zhongshan Station (Fig. 5b). In the enlarged area of the intersection (Fig. 5d), we select the ICESat-2 ice surface points (ATL06) and photons (ATL03) along track 2R (~80 m for ATL06 and ~40 m for ATL03). Specifically, we select the ATL06 points with their quality tag "*atl06_quality_summary"* equal to 0 (no likely problems) and the ATL03 photons with their confidence tag "*signal_conf_ph"* equal to 3 (medium) and 4 (high) to ensure high data quality; we also consider the ATL03 photons with "*signal_conf_ph"* equal to 1 (buffer) and 2 (low) if additional qualified photons are needed (Brunt et al., 2019b). Furthermore, these should be collected within 30 days of the GNSS campaign period to avoid significant changes of the ice surface and other environmental conditions between the two data sets. On the other hand, in order to estimate the ice surface elevations ($H_{Ice\ surface}$) at the GNSS traverse points using Equation (1), the height from the snowcat to the ice surface (h_2) is measured at the locations when the snowcat stops during campaign breaks. At other traverse points between these direct ice surface measurements, we interpolate the values of h_2 using inverse distance weighting (IDW).

https://doi.org/10.5194/tc-2020-330
Preprint. Discussion started: 25 November 2020

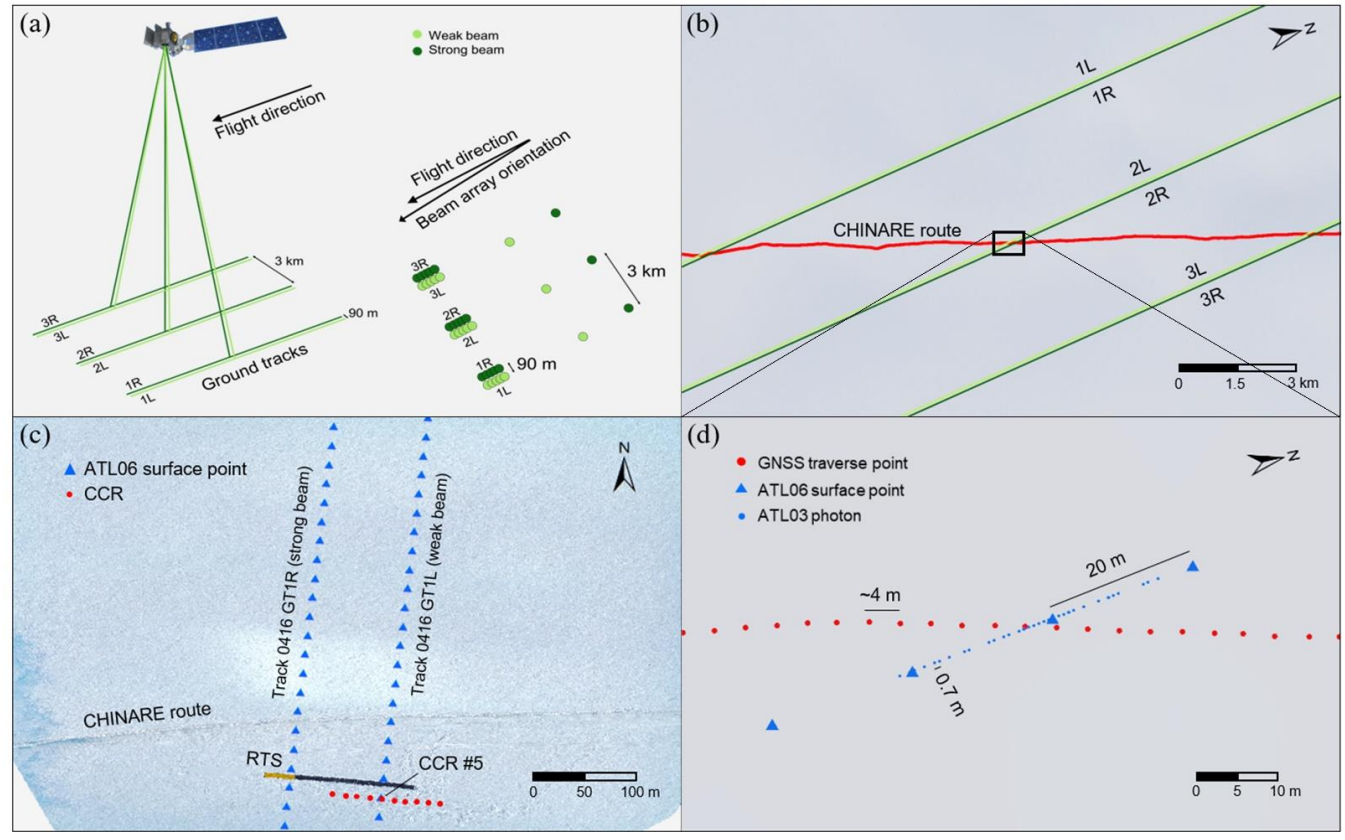

Figure 5. (a) ICESat-2 ground tracks and beam pattern, modified from ICESat-2 Technical Specs (2020), (b) Ground tracks intersecting the CHINARE route (red line) at ~420 km from Zhongshan Station, (c) UAV-DEM mapping area and two ground tracks near Zhongshan Station with a UAV orthophoto as background, and (d) ATL06 ice surface points and ATL03 photons (track 2R) and GNSS traverse points in the enlarged area of the rectangle in (b).

Within an intersection area (Fig. 5d), the elevations of the GNSS traverse points are compared with the ICESat-2 ATL06 and ATL03 data. First, at each ATL06 ice surface point we open a 20 m radius circle inside which there should be at least five GNSS points. We then calculate the difference between the ATL06 point elevation and the median ice surface elevation of the GNSS points. Secondly, for each ATL03 photon we find its nearest GNSS point within a 4 m wide search window to form a pair and calculate their elevation difference. Finally, if the number of pairs is sufficient (≥ 30), we use the median among them to be the representative elevation difference between the ATL03 and GNSS data at this intersection.

3.2 Validation of ICESat-2 photons using CCR and RTS elevations

Design of a photon-capturing CCR array requires a number of considerations. The spacecraft orbiting and sensor pointing capability has been improved after the initial mission (Brunt et al., 2019a). Our preliminary analysis of Releases 001 and 002 data indicated that the offsets between the actual and reference ground tracks in the study area were reduced from up to ~3000 m during the initial mission to 1–6 m before our expedition. Given a footprint of ~13 m diameter every ~0.7 m along the track

https://doi.org/10.5194/tc-2020-330
Preprint. Discussion started: 25 November 2020

(Markus et al., 2017; ICESat-2 Technical Specs, 2020), ICESat-2 measured ~4 photons for weak beams and ~10 photons for strong beams per pulse in our study area; with a CCR field of view (FOV) of ±35 °(see Appendix A), a single line CCR array across a track ensures along-track photon capture. In the cross-track direction we installed 10 CCRs spaced every ~10 m across one weak (or strong) beam track (Fig. 5c); this ensures that at least one CCR is placed inside a footprint of ~13 m along one track. Each CCR has a unique elevation for distinguishing the target CCR from other CCRs (Fig. 4b). The elevation of the CCR pole top ($h_{Pole\ top}$) is surveyed by using the precision RTK GNSS positioning method; then, the height from the CCR center, marked by the manufacturer as the theoretical photon bounce point, to the CCR pole top (dh_{CCR}) is measured using a steel tape. Thus, the elevation of the CCR is estimated as $h_{CCR} = h_{Pole\ top} + dh_{CCR}$. The field deployment and survey are carried out a few hours before the expected satellite pass to avoid severe sinkage of the CCR.

Once the photons are reflected from a CCR and received by ATLAS, a streak of photons along a track with the elevation close to the GNSS-surveyed elevation can be detected in the ICESat-2 ATL03 data (Figs. 6a). We use the photons in the central section of the streak (one footprint long; red rectangles in Fig. 6a and 6c) where the photons are generally of high quality and have the confidence tag "*signal_conf_ph*" equal to 3 or 4 used to calculate an average elevation in each pulse to reduce noises and potential atmospheric effect (blue dots in Fig. 6b). The average elevations are then further fitted to a symmetric curve, e.g., a Gaussian curve. The central point (or peak) of the curve is treated as the representative CCR photon position. An offset is then calculated between the positions estimated from the ATL03 photons and the GNSS survey.

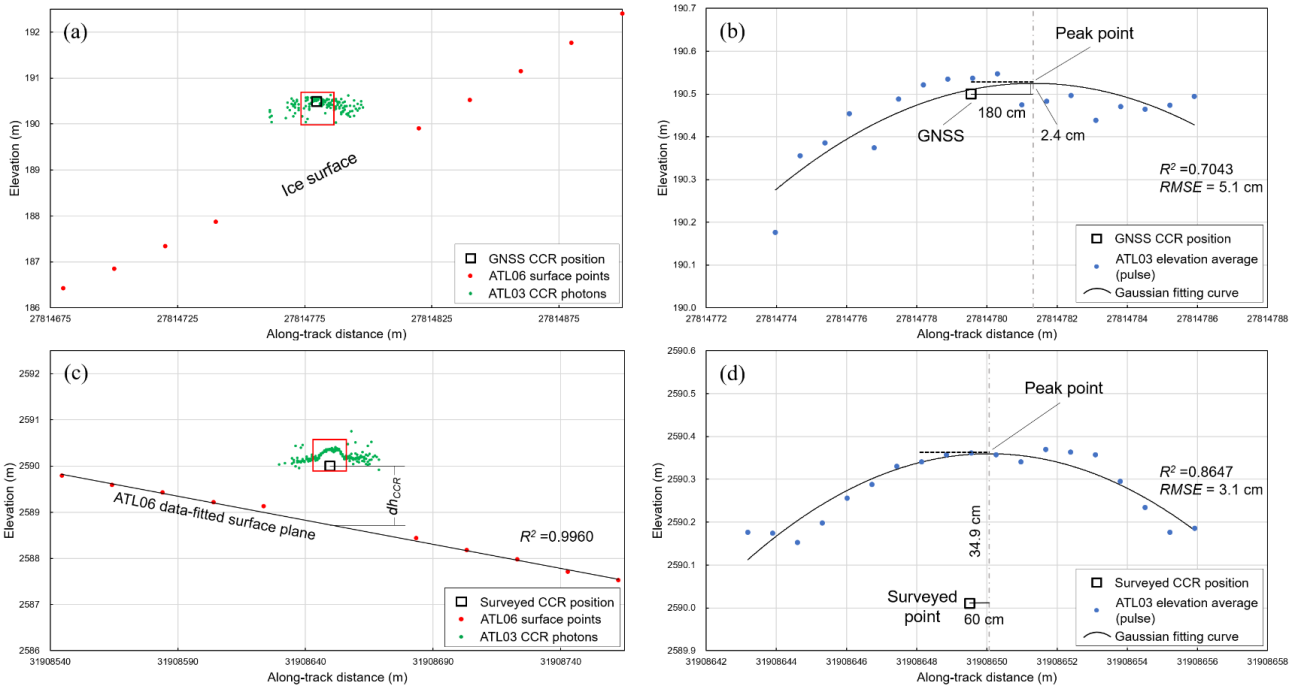

Figure 6. (a) CCR experiment near Zhongshan Station: returned photon streak (ATL03) from CCR #5, GNSS-surveyed CCR position, and ice surface points (ATL06); (b) elevations averaged in each pulse in the red rectangle in (a) to compare with the GNSS-surveyed position; (c) CCR experiment near Taishan Station: returned photon streak (ATL03) from CCR #6, steel tape-surveyed

https://doi.org/10.5194/tc-2020-330
Preprint. Discussion started: 25 November 2020

CCR position, and ice surface points (ATL06); and (d) elevations averaged in each pulse in the red rectangle in (c) to compare with the GNSS-surveyed position.

3.3 Validation of ICESat-2 ice surface elevations using UAV-DEM

To georeference the UAV images, GNSS observations are taken using the D-RTK GNSS mobile station (https://www.dji.com/cn/d-rtk-2?site=brandsite&from=nav) near Zhongshan Station during the image acquisition. This mobile station and other three ground control points (GCPs) are used in GNSS RTK processing to achieve an accuracy of better than 1.0 cm. We generate a UAV-DEM and an orthophoto from the UAV data by using the structure-from-motion multi-view stereo (SfM-MVS) algorithm (James and Robson, 2012; Turner et al., 2014) implemented in the Pix4Dmapper software (version 4.5.6, https://support.pix4d.com/hc/en-us/categories/360001503192-Pix4Dmapper). The accuracy of the produced UAV-DEM and orthophoto is 0.9 cm and 2.3 cm in the horizontal and vertical directions, respectively.

Thereafter, we evaluate the elevation differences ΔH between the elevations of the ICESat-2 ATL06 ice surface points ($H_{Ice\ surface}$) that fall in the UAV-DEM (H_{UAV_DEM}):

$$\Delta H = H_{Ice\ surface} - H_{UAV\_DEM}. \quad (3)$$

At Taishan Station, however, owing to the lack of GCPs and the D-RTK GNSS mobile station, the accuracy of the UAV-derived products is estimated to be several meters and cannot be used for ICESat-2 ice surface elevation validation.

4 Results

4.1 Kinematic GNSS – ICESat-2 ice surface elevation validation

The elevation precision values given by the GNSS PPP processing software system for the five base stations, from Base 1 to Base 5, are at the sub-centimeter (0.5 cm, 0.9 cm, 0.8 cm, 0.7 cm, and 0.9 cm) level. For the positions of the roof-mounted GNSS receivers along the inbound and outbound traverses, a threshold of the precision values given by the kinematic GNSS RTK positioning software system was used to filter out traverse points with large errors originating from rough terrain features and other noises, i.e., 3σ for the undulated topography near the coast (0–67 km) and 2σ for the relatively flat inland topography (67–520 km). As a result, a total of 625,358 GNSS traverse points were obtained, which have an average internal elevation precision of 1.6 ±0.6 cm given by the software system. Finally, the elevation accuracy of the GNSS traverse was assessed as 0.1 ±5.5 cm by using 27 crossovers of the traverse itself (Fig. 2c) where the GNSS surveyed elevations from two intersecting traverse segments were compared.

There were 20 locations along the traverse (Fig. 1) where h_2 was measured (Fig. 4a). Along with the other two bore sight parameters, h_0 and h_1, these direct measurements were used to derive the ice surface elevations $H_{Ice\ surface}$ from the roof-mounted kinematic GNSS observations H_{GNSS}. The average of the measured h_2 is 93.0 cm with a standard deviation of 3.2 cm. This variation is mainly attributed to the microtopography and firn density changes at different locations along the 520

https://doi.org/10.5194/tc-2020-330
Preprint. Discussion started: 25 November 2020


The Cryosphere Discussions

km traverse from the coast to the highland interior. Out of the 134 intersections between the GNSS traverse and ICESat-2 tracks, we selected 25 intersections that are within 2 km of the h_2 direct measurement locations to enhance the comparability between the elevations observed by the ICESat-2 satellite and the kinematic GNSS receivers along the traverse. The average distance between the intersections and measurements is ~816 m. We validated the elevations of the ICESat-2 ATL06 ice surface points and ATL03 photons using the GNSS-surveyed elevations that are summarized according to six ICESat-2 tracks separately (Table 2).

Table 2. Assessment of ICESat-2 ATL06 ice surface points and ATL03 photons using the GNSS RTK technique with direct ice surface measurements (h_2) along the 36th CHINARE traverse. Bias and precision were estimated from their elevation differences using N ice surface points or photons. The difference is calculated as ICESat-2 elevation minus GNSS elevation.

Ground track	ATL06 bias ± precision (cm)	ATL03 bias ± precision (cm)
GT1L	+2.2 ± 10.4 (N = 42)	+5.3 ± 5.0 (N = 735)
GT1R	+1.3 ± 8.2 (N = 38)	-0.5 ± 5.9 (N = 1392)
GT2L	+8.1 ± 6.8 (N = 2)	——
GT2R	-5.0 ± 10.3 (N = 3)	——
GT3L	-4.1 ± 9.9 (N = 16)	-2.8 ± 8.6 (N = 366)
GT3R	-3.4 ± 10.2 (N = 14)	-7.6 ± 15.4 (N = 949)
ALL	+1.1 ± 9.7 (N = 115)	+3.7 ± 9.1 (N = 3442)

Compared to the kinematic GNSS elevation observations, the ATL06 ice surface points have median elevation differences (bias) for the six ICESat-2 tracks ranging from -5.0 cm to 8.1 cm and precision values (1σ) ranging from 6.8 cm to 10.4 cm, resulting in an overall bias of 1.1 cm and precision of 9.7 cm. Similarly, the ATL03 photons have an overall bias of 3.7 cm and precision of 9.1 cm. Note that due to the 2 km limit from the direct ice surface measurements h_2 for the selection of intersections, there are no comparison results for the ATL03 tracks of GT2L and GT2R. No significant elevation differences were found between the tracks of the weak and strong beams. Thus, the processed ATL06 application product (L3A Land Ice Height data) has a smaller bias of 1.1 cm than that of 3.7 cm for the unprocessed ATL03 product (L2A Global Geolocated Photon Data), although their precision values are almost the same (9.7 cm and 9.1 cm, respectively).

We further extended our assessment to all intersections of the ICESat-2 tracks and the GNSS traverse without the above 2 km selection limit. At each intersection, the h_2 value was calculated between two measurement locations using the IDW interpolation method. As shown in Table B1, the ATL06 data also present a bias of 0.5 cm, smaller than 3.7 cm for the ATL03 data, which are comparable to these in Table 2. However, the overall precision values of 15.7 cm (ATL06) and 14.2 cm (ATL03) in Table B1 are significantly larger than 9.7 cm (ATL06) and 9.1 cm (ATL03) in Table 1, mainly due to the uncertainty caused by the interpolated h_2 value.

https://doi.org/10.5194/tc-2020-330
Preprint. Discussion started: 25 November 2020

4.2 Validation of ICESat-2 photon elevations using CCRs and RTSs

ICESat-2 passed across the line array of 10 CCRs near Zhongshan Station along orbit 0416 at 23:49 UTC on January 22, 2020 (Fig. 5c). Around 6 h before the ICESat-2 pass, the CCRs were deployed and GNSS was surveyed with an accuracy of 0.3 cm (horizontal) and 0.4 cm (vertical), respectively. A GNSS sinkage survey was performed over 2 days and estimated a negligible sinkage of less than 1 cm. The ATL03 data showed a streak of 137 photons in 40 pulses, spanning ~35 m along the weak beam track (1L; green dots in Fig. 6a). We selected 68 photons of 18 pulses located in the central part of the streak (~13 m, inside the red rectangle). Both the track location and elevations of the photons matched those of CCR #5 (black square), suggesting that it was illuminated during the ICESat-2 pass. The elevations of the photons within each pulse were averaged and used to fit a Gaussian function curve with an R^2 of 0.7043 and a fitting RMSE of 5.1 cm (Fig. 6b), whose peak point was used as the position of the representative photon of the CCR. The offset between the peak point and the GNSS-surveyed position is 180.0 cm in the horizontal direction and 2.4 cm in the vertical direction. On the other hand, ICESat-2 passed across the CCR line array near Taishan Station along orbit 0424 at 12:37 UTC on January 23, 2020. The CCR positions were surveyed through a single-point positioning GNSS survey at an accuracy of 1–2 m in both the horizontal and vertical directions. Based on its horizontal location and the ATL03 data, CCR #6 was found to have returned 176 photons in 51 pulses from the weak beam track (2L; ~38 m, green dots in Fig. 6c). To estimate a CCR elevation h_{CCR} (Fig. 4b) that is more accurate than the meter-level GNSS result, we first used 10 ATL06 ice surface points (red dots in Fig. 6c) to fit a terrain surface plane with an R^2 of 0.9960. Using the approximate GNSS-surveyed CCR location and the fitted ice surface, the improved CCR elevation h_{CCR} (black square) was calculated from the measured pole height dh_{CCR}. After that, the photons were averaged within each of pulse (blue dots in Fig. 6d) to fit another Gaussian function with an R^2 of 0.8647 and an RMSE of 3.1 cm. The peak position of the Gaussian function was used as the representative photon of the CCR that has an offset of 60.0 cm in the horizontal direction and 34.9 cm in the vertical direction from the estimated CCR location.

ICESat-2 passed across the RTS and the CCR line array along the same orbit at each site near Zhongshan Station and Taishan Station, respectively. The combinations of the strong and weak beams and different coatings are listed in the first column of Table 3. There are seven check points on the yellow sheet near Zhongshan Station, which were surveyed using the GNSS RTK method with an accuracy of 0.4 cm. Pairing of the check points with the corresponding ATL03 photons was achieved with a maximum in-between distance of 1.22 m. The comparison between the two datasets resulted in an elevation uncertainty of 2.5 ± 2.7 cm.

The three deployed RTS coatings were tested prior to the Antarctic expedition and their reflectivity was measured as 0.532 for yellow, 0.235 for silver–gray, and 0.060 for dark green coatings, respectively (Table 3). The 5 m wide, high-reflectivity yellow coating reflected photons from the strong beam. There were 183 and 132 ATL03 photons reflected within the footprint containing the RTS near Zhongshan Station and Taishan Station, respectively. Furthermore, the full saturation fraction (FSF) tag "*full_sat_fract*", ranging from 0 to 1, represents the ratio of fully saturated pulses over a 20 m along-track segment (Neumann et al., 2020a). As shown in Table 3, FSF of the two yellow coatings at the two sites are 0. For comparison, the

https://doi.org/10.5194/tc-2020-330
Preprint. Discussion started: 25 November 2020

similar number averages of received photons (149 and 144) and FSF values of 0 were estimated over the 300 m bare ice surface segments next to the RTS for the same strong beam tracks. Therefore, the footprints of the high-reflectivity yellow coating RTSs showed similar photon reflectivity characteristics to the bare ice surface. On the other hand, the two lower-reflectivity coatings, i.e., silver–gray and dark green coatings, reflected photons from the weak beam, but showed higher FSF values (0.321 and 0.429). We suggest that this abnormal phenomenon be attributed to contamination by the photons reflected from the illuminated CCRs, which were only ~9 m away from the RTSs (Fig. 5c).

Table 3. Received photons and full saturation fractions (FSF) with respect to different RTS coatings.

RTS coating (ICESat-2 beam, site)	**Pre-expedition reflectivity**	**No. of received photons (RTS)**	**Full saturation fraction (RTS)**	**No. of received photons (firn)**	**Full saturation fraction (firn)**
Yellow (strong beam, Zhongshan)	0.532	183	0	149	0
Yellow (strong beam, Taishan)	0.532	132	0	144	0
Silver–gray (weak beam, Zhongshan)	0.235	137 (CCR)	0.321 (CCR)	36	0.009
Dark green (weak beam, Taishan)	0.060	191 (CCR)	0.429 (CCR)	44	0.043

In summary, one CCR of the precisely GNSS-surveyed line CCR array near Zhongshan Station was illuminated. The estimated representative CCR photon has an offset of 2.4 cm in elevation and 180.0 cm in horizontal direction from the GNSS-surveyed CCR position. Seven precisely GNSS-surveyed check points that are evenly distributed on a highly reflective RTS near Zhongshan Station were used to validate the elevations of their corresponding ATL03 photons (strong beam) and resulted in a bias and precision of 2.5 ± 2.7 cm.

4.3 Validation of ICESat-2 ice surface elevations using UAV-DEM

The 750 m × 500 m UAV-DEM mapping area near Zhongshan Station contains the RTS and CCR line array (Fig. 5c). ICESat-2 orbit 0416 passed through the area 8 h before the UAV image acquisition. First, 167 check points on the RTS were GNSS surveyed at an elevation accuracy of 0.4 cm and used for the UAV-DEM accuracy assessment. The generated UAV-DEM elevations were compared against those of the check points and achieved an elevation uncertainty of 0.2 ± 6.3 cm. Second, the 1L (weak beam) and 1R (strong beam) tracks have 48 ATL06 ice surface points in the DEM area, among which three were affected by the photons from the CCR and excluded from the validation. The elevation differences between the ATL06 ice surface points and the UAV-DEM were computed and resulted in an estimated ICESat-2 ice surface elevation uncertainty of 1.1 ± 4.9 cm.

https://doi.org/10.5194/tc-2020-330
Preprint. Discussion started: 25 November 2020


The Cryosphere Discussions

5 Discussions

The validation of ICESat-2 elevations at crossovers between the ground tracks and the CHINARE route using a kinematic GNSS positioning technique and direct ice surface measurements produced an elevation bias and precision of 1.1 ±9.7 cm for the ATL06 ice surface points, compared to 3.7 ± 9.1 cm for the ATL03 photons (Table 2). This indicated that the method used for estimating the ice surface elevations every 20 m along a track in ATL06 data (Smith et al., 2019) may be able to significantly reduce the bias, i.e., a reduction of bias from 3.7 cm to 1.1 cm as demonstrated in this study. The precision remained at an approximately same level (⩽ 9.7 cm) and may be mainly caused by the variation of h_2 in Equation (2), the height from the snowcat to ice surface. Although the average distance between the direct h_2 measurements and the crossovers is limited to ~816 m, the factors that influence the pairing of h_2 with the kinematic GNSS positions may include the local microtopography and uneven firn properties from the coast to the interior of Antarctica along the GNSS traverse. This trend is further evidenced in the results by extending the assessment to all crossovers with both directly measured and interpolated h_2 values (Table B1) where the bias can be similarly reduced from 3.7 cm for the ATL03 photons to 0.5 cm for the ATL06 ice surface points. However, the precision decreased (that is, the values increased) from less than 9.7 cm for the experiment using only the directly measured h_2 (Table 2) to less than 15.7 cm for the experiment with interpolated h_2. An improvement of the validation system using continuous measurements of h_2 along the GNSS traverse is planned for experiments in future expeditions.

The accuracy of the ATL03 data was better validated by using targeted photons returned from CCRs and RTSs. One precisely GNSS-surveyed CCR was illuminated by a weak beam and showed an offset of 2.4 cm between the GNSS elevation and that of the representative CCR photon. Furthermore, seven precisely GNSS-surveyed check points on an RTS were compared with the corresponding ATL03 photons and presented a bias and precision of 2.5 ±2.7 cm.

The fact that the photons returned from the CCRs are saturated is indicated by the full saturation fraction (FSF) values of 0.429 and 1.000 for the segments containing the illuminated CCRs near Zhongshan Station and Taishan Station, respectively (Table 4). They are drastically higher than those of their ice surface areas nearby (0.009 and 0.043). It is also noted that the CCR FSF at Zhongshan Station is more than 50% lower than that at Taishan Station (max. FSF). A similar trend exists between FSFs of the ice surface areas at the two sites despite the variation in the ratio. These consistent FSF differences between the two sites may be explained by their corresponding "total neutral atmospheric delay" (TNAD) in the ATL03 data (*/gtx/geolocation/neutat_delay_total*), which represents the totally neutral atmospheric delay correction (Neumann et al., 2020a); TNAD is dependent on the state of the atmosphere, which itself is dependent on the total pressure, partial pressure of water vapor, and air temperature. The TNAD of 2.353 m at Zhongshan Station over that of 1.726 at Taishan Station suggested that atmospheric conditions may have had a severe impact on the CCR photons at Zhongshan Station, including the increased level of refraction and thus, prolonged the time delay of the returned photons. Therefore, we see less-saturated photons (lower FSF) near Zhongshan Station. And the elevations of the CCR photons at Zhongshan Station are also more dispersed (Fig. 6a) compared to the regularly distributed pattern at Taishan Station (Fig. 6c).

https://doi.org/10.5194/tc-2020-330
Preprint. Discussion started: 25 November 2020


The Cryosphere Discussions

Table 4. The full saturation fraction (FSF) and total neutral atmospheric delay (TNAD) of the illuminated CCRs near Zhongshan Station and Taishan Station.

ICESat-2 beam (site)	FSF of CCR (ratio)	FSF of ice surface (ratio)	TNAD of CCR (m)	TNAD of ice surface (m)
Weak beam (Zhongshan)	0.429	0.009	2.335	2.335
Weak beam (Taishan)	1.000	0.043	1.726	1.726

6 Conclusions

This paper presents the results of the assessment of ICESat-2 ice surface elevations along the CHINARE route in East Antarctica. The validation campaign was designed and implemented in cooperation with the 36th CHINARE Antarctic expedition. An assessment of the ICESat-2 ATL03 and ATL06 data was performed along the 520 km traverse using a kinematic GNSS positioning technique. Near Zhongshan Station and Taishan Station, additional coordinated multi-sensor observations of a CCR line array, an RTS, and a UAV were acquired for each site. Overall, this systematic validation of the ICESat-2 data covered a variety of the eastern AIS conditions from the coast to inland Antarctica along the 520 km traverse and is complementary to the 750 km traverse validation of flat inland Antarctica along the latitude of 88°S (Brunt et al., 2020b).

The following conclusions are drawn from this research.

1) The comparison of the ICESat-2 Release 003 data with the high-precision GNSS survey and direct snowcat-to-ice surface height measurements along the 520 km CHINARE route showed that the elevations of the ATL06 ice surface points are accurate to 1.1 cm with 9.7 cm precision (1.1 ± 9.7 cm), and the elevations of the ATL03 photons are accurate to 3.7 cm with 9.1 cm precision (3.7 ± 9.1 cm). This is comparable to the similar result of the ICESat-2 Release 001 data validation, 3 ± 9 cm for the ATL06 data and 5 ± 13 cm for the ATL03 data along a traverse of the 88 °S parallel (Brunt et al., 2019b).
2) The validation of the ATL06 ice surface points along two ICESat-2 tracks with a high-precision GNSS-controlled UAV-DEM (750 m × 500 m) near Zhongshan Station indicated that the ATL06 elevations are accurate to 1.1 cm with 4.9 cm precision. Although the DEM coverage is relatively small, these validation results show the potentially achievable accuracy using the ICESat-2 ATL06 data in many applications in the AIS environment.
3) The validation of the ICESat-2 ATL03 data using a high-precision GNSS-surveyed CCR showed an accuracy of 2.4 cm. An additional experiment using seven high-precision GNSS-surveyed check points on the RTS near Zhongshan Station indicated that the ATL03 data are accurate to 2.5 cm with 2.7 cm precision. This suggests that an assessment using targeted and controlled (or partially) photons can result in high elevation accuracy.

https://doi.org/10.5194/tc-2020-330
Preprint. Discussion started: 25 November 2020

Overall, our ICESat-2 data validation results show that the elevation of the ATL06 ice surface points is accurate to 1.1 cm with a precision ranging from 4.7 cm in a local UAV-DEM environment near Zhongshan Station to 9.7 cm along the 520 km CHINARE route. The elevation of the ATL03 photons is accurate to 2.4 cm as estimated by using a line array of CCRs, and accurate to 2.5 cm with 2.7 cm precision as estimated by using RTSs. The validation results demonstrated that the estimated ICESat-2 elevations are accurate to 1.1–2.5 cm in this East Antarctic region, which is higher than prior satellite altimeters and important for overcoming the difficulties in estimation of mass balance in East Antarctica, as well as useful for other Antarctic applications. Our ICESat-2 validation methodology and sensor system will be improved to carry out the continued assessment of the ICESat-2 data, especially ATLAS performance during its later operation period.

Data availability. The ICESat-2 data were downloaded from the NASA National Snow and Ice Data Center (NSIDC).

Author contributions. RL led the study and designed the cal-val campaign. TH and GQ carried out field observations. All authors were involved in data processing, analysis and presentation.

Competing interests. The authors declare that they have no conflict of interest.

Acknowledgements. The logistic and technical support provided by the 36th CHINARE team and the Polar Research Institute of China is appreciated. This study was supported by the National Science Foundation of China (41730102).

https://doi.org/10.5194/tc-2020-330
Preprint. Discussion started: 25 November 2020

References

Bindschadler, R., Vornberger, P., Fleming, A., Fox, A., Mullins, J., Binnie, D., Paulsen, S. J., Granneman, B., and Gorodetzky, D.: The Landsat image mosaic of Antarctica, Remote Sens. Environ., 112, 4214-4226, https://doi.org/10.1016/j.rse.2008.07.006, 2008.

Born, M., Clemmow, P., Gabor, D., Stokes, A., Taylor, A., Wayman, A., Wilcock, W., and Wolf, E. (Eds.): Principles of Optics, 7th (expanded) edition, Pergamon Press, Oxford, Britain, 1999.

Brunt, K. M., Hawley, R. L., Lutz, E. R., Studinger, M., Sonntag, J. G., Hofton, M. A., Andrews, L. C., and Neumann, T. A.: Assessment of NASA airborne laser altimetry data using ground-based GPS data near Summit Station, Greenland, The Cryosphere, 11(2), 681–692, https://doi.org/10.5194/tc-11-681-2017, 2017.

Brunt, K. M., Neumann, T. A., and Larsen, C. F.: Assessment of altimetry using ground-based GPS data from the 88S traverse, Antarctica, in support of ICESat-2, The Cryosphere, 13(2), 570-590, https://doi.org/10.5194/tc-13-579-2019, 2019a.

Brunt, K. M., Neumann, T. A., and Smith, B. E.: Assessment of ICESat-2 ice sheet surface heights, based on comparisons over the interior of the Antarctic ice sheet, Geophys. Res. Lett., 46(22), 13072-13078, https://doi:10.1029/2019GL084886, 2019b.

Hartzell, P., Dang, Z., Pan, Z., and Glennie, C.: Radiometric evaluation of an airborne single photon Lidar sensor, IEEE Geosci. Remote S., 15(9), 1466-1470, https://doi.org/10.1109/LGRS.2018.2841811, 2018.

ICESat-2 Technical Specs,: https://icesat-2.gsfc.nasa.gov/science/specs, last access: 27 September 2020.

James, M. R., and Robson, S.: Straightforward reconstruction of 3D surfaces and topography with a camera: accuracy and geoscience application, J. Geophys. Res., 117, F03017, https://doi.org/10.1029/2011JF002289, 2012.

Kohler, J., Neumann, T. A., Robbins, J. W., Tronstad, S., and Melland, G.: ICESat elevations in Antarctica along the 2007-09 Norway-USA Traverse: validation with ground-based GPS, IEEE T. Geosci. Remote, 51(3), 1578-1587, http://doi.org/10.1109/TGRS.2012.2207963, 2013.

Li, B., Zang, N., Ge, H., and Shen, Y.: Single-frequency PPP models: analytical and numerical comparison, J. Geod., 93(12): 2499-2514, https://doi.org/10.1007/s00190-019-01311-4, 2019.

Magruder L. A., and Brunt K. M.: Performance analysis of airborne photon-counting lidar data in preparation for the ICESat-2 mission, IEEE T. Geosci. Remote, 56(5), 2911-2918, https://doi.org/10.1109/TGRS.2017.2786659, 2018.

Markus, T., Neumann, T., Martino, A., Abdalati, W., Brunt, K., Csatho, B., Farrell, S., Fricker, H., Gardner, A., Harding, D., Jasinski, M., Kwok, R., Magruder, L., Lubin, D., Luthcke, S., Morison, J., Nelson, R., Neuenschwander, A., Palm, S., Popescu, S., Shum, B. E., Schutz, R., Smith, B., Yang, Y., and Zwally, J.: The Ice, Cloud, and Land Elevation Satellite-2 (ICESat-2): Science requirements, concept, and implementation, Remote Sens. Environ., 190, 260-273, https://doi.org/10.1016/j.rse.2016.12.029, 2017.

National Research Council: Earth science and applications from space: national imperatives for the next decade and beyond, the national academies press, Washington, D.C, https://doi.og/10.17226/11820, 2007.

Neumann, T., Brenner, A., Hancock, D., Harbeck, K., Luthcke, S., Robbins, J., Saba, J., and Gibbons, A.: Ice, Cloud, and Land Elevation Satellite-2 project algorithm theoretical basis document for global geolocated photons (ATL03), https://icesat-2.gsfc.nasa.gov/science/data-products, last access: 27 September 2020, 2018.

Neumann, T. A., Martino, A. J., Markus, T., Bae, S., Bock, M. R., Brenner, A. C., Brunt, K. M., Cavanaugh, J., Fernandes, S. T., Hancock, D. W., Harbeck, K., Lee, J., Kurtz, N. T., Luers, P. J., Luthcke, S. B., Magruder, L., Pennington, T. A., Ramos-Izquierdo, L., Rebold, T., Skoog, J., and Thomas, T. C.: The Ice, Cloud, and Land Elevation Satellite-2 Mission: A global geolocated photon product derived from the Advanced Topographic Laser Altimeter System, Remote Sens. Environ., 233, 111325, https://doi.org/10.1016/j.rse.2019.111325, 2019.

Neumann, T., Brenner, A., Hancock, D., Robbins, J., Saba, J., Harbeck, K., Gibbons, A., Lee, J., Luthcke, S., and Rebold, T.: ATLAS/ICESat-2 L2A global geolocated photon data, Version 3, NASA National Snow and Ice Data Center, Distributed Active Archive Center, Boulder, Colorado USA, https://doi.org/10.5067/ATLAS/ATL03.003, last access: 4 August 2020, 2020a.

Neumann, T., Brunt, K., Marguder, L., and Kurtz, N.: Validation activities for the Ice, Cloud, and Land Elevation Satellite - 2 (ICESat-2) Mission, EGU General Assembly 2020, Online, 4–8 May 2020, EGU2020-20671, https://doi.org/10.5194/egusphere-egu2020-20671, 2020b.

Richter, A., Horwath M., and Dietrich R.: Comment on Zwally and others (2015) - Mass gains of the Antarctic ice sheet exceed losses, J. Glaciol., 1.233, 1-3, https://doi.org/10.1017/jog.2016.60, 2016.

Scambos, T., and Shuman C.: Comment on 'Mass gains of the Antarctic ice sheet exceed losses' by H. J. Zwally and others, J. Glaciol., 1.233, 1-5, https://doi.org/10.1017/jog.2016.59, 2016.

Schutz, B. E., Bae, S., Smith, N., and Sirota, M.: Precision orbit and attitude determination for ICESat, Adv. Astronaut. Sci, 115, 416-427, 2008.

Smith, B., Fricker, H. A., Holschuh, N., Gardner, A. S., Adusumilli, S., Brunt, K. M., Csatho, B., Huth, A., Neumann, T., Nilsson, J., and Siegfried, M. R.: Land ice height-retrieval algorithms for NASA's ICESat-2 photon-counting laser altimeter, Remote Sens. Environ., 233, 111352, https://doi.org/10.1016/j.rse.2019.111352, 2019.

Smith, B., Fricker, H. A., Gardner, A. S., Medley, B., Nilsson, J., Paolo, F. S., Holschun, N., Adusumilli, S., Brunt, K., Csatho, B., Harbeck, K., Markus, T., Neumann, T., Siegfried, M. R., and Zwally, H. J.: Pervasive ice sheet mass loss reflects competing ocean and atmosphere processes, Science, 368(6496), 1239-1242, https://doi.org/10.1126/science.aaz5845, 2020.

Takasu, T. and Yasuda, A.: Development of the low-cost RTK-GPS receiver with an open source program package RTKLIB, International Symposium on GPS/GNSS, International Convention Center Jeju, Korea, November 4-6, 2009.

Takasu, T.: RTKLIB ver. 2.4.2 Manual, http://www.rtklib.com/prog/manual_2.4.2.pdf, last access: 21 October 2020, 2013.

Turner, D., Lucieer, A., and Wallace, L.: Direct georeferencing of ultrahigh-resolution UAV imagery, IEEE T. Geosci. Remote, 52(5):2738-2745, https://doi.org/10.1109/TGRS.2013.2265295, 2014.

https://doi.org/10.5194/tc-2020-330
Preprint. Discussion started: 25 November 2020

Zwally, H. J., Schutz, B., Abdalati, W., Abshire, J., Bentley, C., Brenner, A., Bufton, J., Dezio, J., Hancock, D., Harding, D., Herring, T., Minster, B., Quinn, K., Palm, S., Spinhirne, J., and Thomas, R.: ICESat's laser measurements of polar ice, atmosphere, ocean, and land, J. Geodyn., 34, 405-445, https://doi.org/10.1016/S0264-3707(02)00042-X, 2002.

Zwally, H. J., Li, J., Robbins, J. W., Saba, J. L., Yi, D., and Brenner, A. C.: Mass gains of the Antarctic ice sheet exceed losses, J. Glaciol., 61.230, 1019-1036, https://doi.org/10.3189/2015JoG15J071, 2015.

https://doi.org/10.5194/tc-2020-330
Preprint. Discussion started: 25 November 2020

480 **Appendices**

Appendix A. CCR lens

The mechanism of photons entering into and reflecting from a CCR is realized according to the optical total reflection principle (Born et al., 1999). The CCR we used is an optical reflector made of K-3 glass
485 (https://detail.1688.com/offer/596318137089.html?spm=a2615.2177701.autotrace-fullscreenImg.4.ffa37343W4lgF8) originally designed for laser distance ranging (Fig. A1a). The lens system consists of three adjacent and mutually orthogonal plane-reflecting surfaces, which have an angle of 54.73 °from the horizontal plane (Fig. A1b). An incident beam ① from the satellite comes out of the CCR as the main outgoing beam ② that is parallel to ① but in the opposite direction, allowing it to be received by the satellite. The system guarantees that any photon from the satellite entering the field of view (FOV) of the
490 CCR, ±35 ° from the zenith, will be returned to the satellite. Ideally, the elevations of all photons returned from the CCR would be placed at one location on the ice surface. However, the ATLAS places all photons collected inside a footprint (~13 m) at one location, which includes those from the CCR and the surrounding area. Therefore, bounded between the first footprint entering the FOV and the last footprint exiting the FOV, the elevations of photons returned from the CCR are recorded as a streak of photons in ATL03 data (green dots in Figs. 6a and 6c).

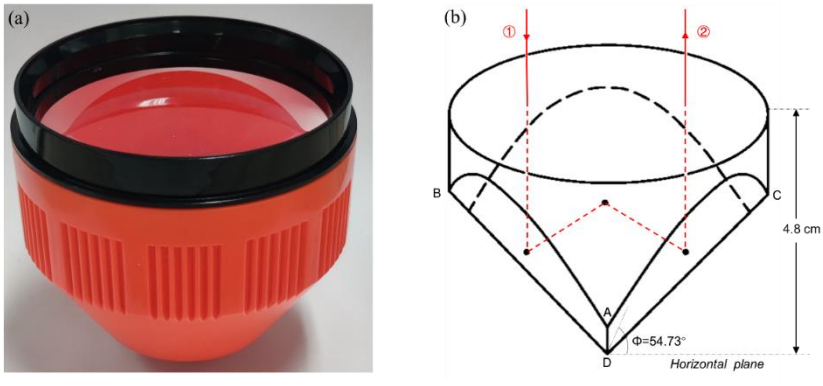

495

Figure A1. (a) CCR head used for calibration of ICESat-2 ATL03 data, and (b) parameters of the lens system and optical path of a total-reflecting photon.

https://doi.org/10.5194/tc-2020-330
Preprint. Discussion started: 25 November 2020


The Cryosphere Discussions
Open Access
EGU

Appendix B. Assessment using observations at all intersections

Table B1. Assessment of ICESat-2 ATL06 ice surface points and ATL03 photons using the GNSS RTK technique at all intersections along the GNSS traverse. Bias and precision were estimated from their elevation differences using N ice surface points or photons. The difference is calculated as ICESat-2 elevation minus GNSS elevation.

Ground track	ATL06 bias ± precision*	ATL03 bias ± precision
GT1L	+3.2 ± 16.5 (N = 114)	+6.8 ± 13.2 (N = 1826)
GT1R	+2.2 ± 16.1 (N = 118)	+4.7 ± 14.6 (N = 4504)
GT2L	+0.2 ± 14.8 (N = 112)	+1.0 ± 12.1 (N = 1324)
GT2R	-1.8 ± 15.9 (N = 115)	+3.5 ± 14.6 (N = 4547)
GT3L	-0.4 ± 14.4 (N = 120)	+2.8 ± 13.6 (N = 1827)
GT3R	-2.6 ± 15.8 (N = 131)	+1.7 ± 15.4 (N = 6285)
ALL	+0.5 ± 15.7 (N = 710)	+3.7 ± 14.2 (N = 20313)